Open Research Online

The LOFT mission concept: a status update

Conference or Workshop Item

For guidance on citations see FAQs.

oro.open.ac.uk

The LOFT mission concept – A status update

M. Feroci[1,1a,1b]; E. Bozzo[3]; S. Brandt[19]; M. Hernanz[6]; M. van der Klis[5]; L.-P. Liu[200]; P. Orleanski[68]; M. Pohl[25]; A. Santangelo[17]; S. Schanne[16]; L. Stella[27]; T. Takahashi[94]; H. Tamura[195]; A. Watts[5]; J. Wilms[87]; S. Zane[29]; S.-N. Zhang[143]; S. Bhattacharyya[132]; I. Agudo[116]; M. Ahangarianabhari[14]; C. Albertus[137]; M. Alford[139]; A. Alpar[4]; D. Altamirano[107]; L. Alvarez[6]; L. Amati[7]; C. Amoros[8]; N. Andersson[9]; A. Antonelli[10]; A. Argan[1]; R. Artigue[8]; B. Artigues[6]; J.-L. Atteia[8]; P. Azzarello[3]; P. Bakala[86]; D. R. Ballantyne[162]; G. Baldazzi[103], M. Baldo[188]; S. Balman[11]; M. Barbera[12,106]; C. van Baren[2]; D. Barret[8]; A. Baykal[11]; M. Begelman[170]; E. Behar[181]; O. Behar[128]; T. Belloni[13]; P. Bellutti[205]; F. Bernardini[161]; G. Bertuccio[14]; S. Bianchi[59]; A. Bianchini[15]; P. Binko[3]; P. Blay[125]; F. Bocchino[99]; M. Bode[169];P. Bodin[114]; I. Bombaci[117]; J.-M. Bonnet Bidaud[16]; G. Borghi[205]; S. Boutloukos[17]; F. Bouyjou[16]; L. Bradley[29]; J. Braga[18]; M.S. Briggs[194]; E. Brown[49]; M. Buballa[191]; N. Bucciantini[21]; L. Burderi[22]; M. Burgay[115]; M. Bursa[23]; C. Budtz-Jørgensen[19]; E. Cackett[111]; F.R. Cadoux[25]; P. Cais[26]; G.A. Caliandro[6]; R. Campana[1,1b]; S. Campana[13]; X. Cao[143]; F. Capitanio[1]; J. Casares[82]; P. Casella[27]; A.J. Castro-Tirado[116]; E. Cavazzuti[10]; Y. Cavecchi[5]; S. Celestin[198]; P. Cerda-Duran[125]; D. Chakrabarty[28]; N. Chamel[192]; F. Château[16]; C. Chen[150]; Y. Chen[143]; Y. Chen[148]; J. Chenevez[19]; M. Chernyakova[197]; J. Coker[29]; R. Cole[29]; A. Collura[106], M. Coriat[8]; R. Cornelisse[82]; L. Costamante[173]; A. Cros[8]; W. Cui[149]; A. Cumming[31]; G. Cusumano[57]; B. Czerny[50]; A. D'Aì[12]; F. D'Ammando[102,103]; V. D'Elia[10]; Z. Dai[148]; E. Del Monte[1,1b]; A. De Luca[85]; D. De Martino[31]; J.P.C. Dercksen[2]; M. De Pasquale[57]; A. De Rosa[1]; M. Del Santo[1]; S. Di Cosimo[1]; N. Degenaar[196]; J.W. den Herder[2]; S. Diebold[17]; T. Di Salvo[12]; Y. Dong[143]; I. Donnarumma[1]; V. Doroshenko[17]; G. Doyle[86]; S.A. Drake[93]; M. Durant[33]; D. Emmanoulopoulos[107]; T. Enoto[93]; M.H. Erkut[135]; P. Esposito[85]; Y. Evangelista[1,1b]; A. Fabian[24]; M. Falanga[34]; Y. Favre[25]; C. Feldman[35]; R. Fender[140]; H. Feng[145]; V. Ferrari[128]; C. Ferrigno[3]; F. Ficorella[205]; M. Finger[133]; M. H. Finger[36]; G.W. Fraser[35]; M. Frericks[2]; M. Fullekrug[199]; F. Fuschino[7]; M. Gabler[125]; D.K. Galloway[37]; J.L. Galvez Sanchez[6]; P. Gandhi[9]; Z. Gao[151]; E. Garcia-Berro[6]; B. Gendre[10]; O. Gevin[16]; S. Gezari[62]; A.B. Giles[39]; M. Gilfanov[40]; P. Giommi[10]; G. Giovannini[102]; M. Giroletti[102]; E. Gogus[4]; A. Goldwurm[105]; K. Goluchová[86]; D. Götz[16]; L. Gou[147]; C. Gouiffes[16]; P. Grandi[7]; M. Grassi[56]; J. Greiner[123]; V. Grinberg[28]; P. Groot[42]; M. Gschwender[17]; L. Gualtieri[128]; M. Guedel[184]; C. Guidorzi[32]; L. Guy[3]; D. Haas[2]; P. Haensel[50]; M. Hailey[29]; K. Hamuguchi[183]; F. Hansen[19]; D.H. Hartmann[42]; C.A. Haswell[43]; K. Hebeler[88,191], A. Heger[37]; M. Hempel[156]; W. Hermsen[2]; J. Homan[28]; A. Hornstrup[19]; R. Hudec[23,72]; J. Huovelin[45]; D. Huppenkothen[203]; S. C. Inam[180]; A. Ingram[5]; J.J.M. in't Zand[2]; G. Israel[27]; K. Iwasawa[20]; L. Izzo[47]; H.M. Jacobs[2]; F. Jetter[17]; T. Johannsen[118,127]; H.M. Jacobs[2]; P.A. Jenke[186]; P. Jonker[2]; J. Josè[126]; P. Kaaret[49]; M. Kalamkar[27]; E. Kalemci[4]; G. Kanbach[123]; V. Karas[23]; D. Karelin[6]; D. Kataria[29]; L. Keek[162]; T. Kennedy[29]; D. Klochkov[17]; W. Kluzniak[50]; E. Koerding[168]; K. Kokkotas[17]; S. Komossa[165]; S. Korpela[45]; C. Kouveliotou[51]; A.F. Kowalski[93]; I. Kreykenbohm[87]; L.M. Kuiper[2]; D. Kunneriath[23]; A. Kurkela[159]; I. Kuvvetli[19]; F. La Franca[59]; C. Labanti[7]; D. Lai[52]; F.K. Lamb[53]; C. Lachaud[105]; P.P. Laubert[2]; F. Lebrun[105]; X. Li[148]; E. Liang[154]; O. Limousin[16]; D. Lin[8]; M. Linares[82,108]; D. Linder[29]; G. Lodato[54]; F. Longo[55]; F. Lu[143]; N. Lund[19]; T.J. Maccarone[131]; D. Macera[14]; S. Maestre[8]; S. Mahmoodifar[93]; D. Maier[17]; P. Malcovati[56]; J. Malzac[8]; C. Malone[175]; I. Mandel[120]; V. Mangano[142]; A. Manousakis[50]; M. Marelli[85]; J. Margueron[158]; M. Marisaldi[7]; S.B. Markoff[5]; A. Markowitz[109]; A. Marinucci[59]; A. Martindale[35]; G. Martinez[191]; I.M. McHardy[107]; G.

[1a] marco.feroci@inaf.it

Medina-Tanco[201]; M. Mehdipour[2]; A. Melatos[60]; M. Mendez[61]; S. Mereghetti[85]; S. Migliari[20]; R. Mignani[29,108]; M. Michalska[68]; T. Mihara[77]; M.C. Miller[62]; J.M. Miller[49]; T. Mineo[57]; G. Miniutti[112]; S. Morsink[64]; C. Motch[65]; S. Motta[140]; M. Mouchet[66]; G. Mouret[8]; J. Mulačová[19]; F. Muleri[1,1b]; T. Muñoz-Darias[140]; I. Negueruela[95]; J. Neilsen[28]; T. Neubert[19]; A.J. Norton[43]; M. Nowak[28]; A. Nucita[167]; P. O'Brien[35]; M. Oertel[158]; P.E.H. Olsen[19]; M. Orienti[102]; M. Orio[99,110]; M. Orlandini[7]; J.P. Osborne[35]; R. Osten[69]; F. Ozel[70]; L. Pacciani[1,1b]; F. Paerels[176]; S. Paltani[3]; M. Paolillo[119]; I. Papadakis[81]; A. Papitto[6]; Z. Paragi[164]; J. M. Paredes[20]; A. Patruno[83,141]; B. Paul[71]; F. Pederiva[187]; E. Perinati[17]; A. Pellizzoni[115]; A.V. Penacchioni[47]; U. Peretz[181]; M.A. Perez[136]; M. Perez-Torres[116]; B.M. Peterson[202]; V. Petracek[72]; A. Picciotto[205]; C. Piemonte[205]; C. Pittori[10]; J. Pons[95]; J. Portell[6]; A. Possenti[115]; K. Postnov[179]; J. Poutanen[73]; M. Prakash[122]; I. Prandoni[102]; H. Le Provost[16]; D. Psaltis[70]; J. Pye[35]; J. Qu[143]; D. Rambaud[8]; P. Ramon[8]; G. Ramsay[76]; M. Rapisarda[1,1b]; A. Rachevski[77]; I. Rashevskaya[206]; P.S. Ray[78]; N. Rea[6]; S. Reddy[80]; P. Reig[113,81]; M. Reina Aranda[63]; R. Remillard[28]; C. Reynolds[62]; L. Rezzolla[124]; M. Ribo[20]; R. de la Rie[2]; A. Riggio[115]; A. Rios[138]; D.H. Rischke[189]; P. Rodríguez-Gil[82,104]; J. Rodriguez[16]; R. Rohlfs[3]; P. Romano[57]; E.M.R. Rossi[83]; A. Rozanska[50]; A. Rousseau[29]; B. Rudak[50]; D.M. Russell[161]; F. Ryde[84]; L. Sabau-Graziati[63]; T. Sakamoto[193]; G. Sala[6]; R. Salvaterra[85]; D. Salvetti[85]; A. Sanna[61]; J. Sandberg[134]; T. Savolainen[165]; S. Scaringi[123]; J. Schaffner-Bielich[189]; H. Schatz[49]; J. Schee[86]; C. Schmid[87]; M. Serino[177]; N. Shakura[179]; S. Shore[117]; J.D. Schnittman[93]; R. Schneider[27]; A. Schwenk[88,191]; A.D. Schwope[89]; A. Sedrakian[189]; J.-Y. Seyler[114]; A. Shearer[90]; A. Slowikowska[172]; M. Sims[35]; A. Smith[29]; D.M. Smith[58]; P.J. Smith[29]; M. Sobolewska[50]; V. Sochora[23]; P. Soffitta[1]; P. Soleri[61]; L. Song[143]; A. Spencer[29]; A. Stamerra[174]; B. Stappers[91]; R. Staubert[17]; A.W. Steiner[204]; N. Stergioulas[92]; A. L. Stevens[5]; G. Stratta[185]; T.E. Strohmayer[93]; Z. Stuchlik[86]; S. Suchy[17]; V. Suleimanov[17]; F. Tamburini[15]; T. Tauris[129]; F. Tavecchio[13]; C. Tenzer[17]; F.K. Thielemann[156]; A. Tiengo[171]; L. Tolos[6]; F. Tombesi[62]; J. Tomsick[121]; G. Torok[86]; J.M. Torrejon[95]; D.F. Torres[96]; E. Torresi[7]; A. Tramacere[3]; I. Traulsen[89]; A. Trois[1]; R. Turolla[15]; S. Turriziani[101], S. Typel[190]; P. Uter[17]; P. Uttley[5]; A. Vacchi[77]; P. Varniere[105]; S. Vaughan[35]; S. Vercellone[57]; M. Vietri[160]; F.H. Vincent[50]; V. Vrba[97]; D. Walton[29]; J. Wang[143]; Z. Wang[146]; S. Watanabe[94]; R. Wawrzaszek[68]; N. Webb[8]; N. Weinberg[28]; H. Wende[17]; P. Wheatley[98]; R. Wijers[5]; R. Wijnands[5]; M. Wille[87]; C.A. Wilson-Hodge[44]; B. Winter[29]; S. J. Walk[182]; K. Wood[78]; S.E. Woosley[58]; X. Wu[155]; L. Xiao[200]; R. Xu[153]; W. Yu[144]; F. Yuan[144]; W. Yuan[147]; Y. Yuan[152]; G. Zampa[77]; N. Zampa[77]; L. Zampieri[99]; L. Zdunik[50]; A. Zdziarski[50]; A. Zech[157]; B. Zhang[100]; C. Zhang[147]; S. Zhang[143]; M. Zingale[178]; N. Zorzi[205]; F. Zwart[2].

[1]IAPS-INAF, Via del Fosso del Cavaliere 100 - 00133 Rome, Italy; [1b]INFN, Sez. Roma Tor Vergata, Via della Ricerca Scientifica 1 - 00133 Rome, Italy; [2]SRON, Sorbonnelaan 2 - 3584 CA Utrecht, The Netherlands; [3]ISDC, Geneve University, Chemin d'Ecogia 16 - 1290 Versoix, Switzerland; [4]Sabanci University, Orhanli-Tuzla 34956, Istanbul, Turkey; [5]Astronomical Institute Anton Pannekoek, University of Amsterdam, Science Park 904 - 1098 XH Amsterdam, The Netherlands; [6]IEEC-CSIC-UPC-UB, Carrer del Gran Capità, 2 - 08034 Barcelona, Spain; [7]INAF-IASF-Bologna, Via P. Gobetti, 101 - 40129 Bologna, Italy; [8]IRAP, avenue du Colonel Roche, 9 - BP 44346 Toulouse, France; [9]Faculty of Physical and Applied Sciences, University of Southampton, Southampton, SO17 1BJ, United Kingdom; [10]ASDC, Via del Politecnico snc - 00133 Rome, Italy; [11]Middle East Technical University, Ankara, Mah. Dumlupınar Blv. No:1 - 06800 Çankaya Ankara, Turkey; [12]Dipartimento di Fisica, Palermo University, Via Archirafi, 36 - 90123 Palermo, Italy; [13]INAF-OA Brera, Via E. Bianchi 46 – 23807 Merate (LC), Italy; [14]Politecnico Milano, Piazza Leonardo da Vinci, 32 - 20133 Milano, Italy; [15]Dept. of Physics and Astronomy University of

Padua, vicolo Osservatorio 3, 35122, Padova, Italy; [16]CEA Saclay, DSM/IRFU/SAp, 91191 Gif sur Yvette, France; [17] IAAT University of Tuebingen, Sand 1 - 72076 Tuebingen, Germany; [18]INPE, Avenida dos Astronautas 1.758, Jd. da Granja - 12227-010 São José dos Campos, Brazil; [19]National Space Institute, Technical University of Denmark, Elektrovej Bld 327, 2800 Kgs Lyngby, Denmark; [20]DAM and ICC-UB, Universitat de Barcelona (IEEC-UB), Martì i Franquès 1, E-08028, Barcelona, Spain; [21]Arcetri Observatory, INAF, Largo Enrico Fermi 5 - I-50125 Firenze, Italy; [22]Cagliari University, Strada provinciale per Sestu, KM 1 - 09042 Monserrato, Italy; [23]Astronomical Institute of the Academy of Sciences of the Czech Republic, Fricova 298, CZ-251 65 Ondrejov, Czech Republic; [24]Cambridge University, Trinity Lane - CB2 1TN Cambridge, United Kingdom; [25]DPNC, Geneve University, Quai Ernest-Ansermet 30 - 1205 Geneva, Switzerland; [26]Laboratoire d'Astrophysique de Bordeaux, rue de l'Observatoire - BP 89 - 33270 Floirac Cedex, France; [27]INAF-OA Roma, Via Frascati, 33 - 00040 Monte Porzio Catone, Italy; [28]MIT, 77 Massachusetts Avenue - MA 02139 Cambridge, United States; [29]MSSL, University College of London, Holmbury St Mary - RH5 6NT Dorking, Surrey, United Kingdom; [30]McGill University, 845 Sherbrooke Street West - QC H3A 0G4 Montréal, Canada; [31]INAF-OA Capodimonte, Salita Moiariello, 16 - 80131 Napoli, Italy; [32]Ferrara University, Via Saragat 1 - 44122 Ferrara, Italy; [33]Department of Medical Biophysics, University of Toronto, M4N 3M5 Canada; [34]ISSI Bern, Hallerstrasse 6 - 3012 Bern, Switzerland; [35]Leicester University, University Road - LE1 7RH Leicester, United Kingdom; [36]Universities Space Research Association, 6767 Old Madison Pike, Suite 450, Huntsville, Alabama 35806, United States; [37] Monash Centre for Astrophysics, School of Physics and School of Mathematical Sciences, Monash University, Clayton VIC 3800, Australia; [38]Johns Hopkins University, 3400 North Charles Street - Baltimore, United States; [39] University of Tasmania, Private Bag 37, Hobart, TAS 7001, Australia; [40]MPA Garching, Karl-Schwarzschild-Str. 1 - 85741 Garching, Germany; [41]Radboud University, Heyendaalseweg 135 - 6500 GL Nijmegen, The Netherlands; [42]Clemson University, Clemson, SC 29634, United States; [43]Open University, Walton Hall - MK7 6AA Milton Keynes, United Kingdom; [44]Astrophysics Office, ZP12, NASA/Marshall Space Flight Center, Huntsville, AL 35812, United States; [45]Department of Physics, Division of Geophysics and Astronomy, P.O. Box 48, FI-00014 University of Helsinki, Finland; [46]Durham University, Stockton Rd - DH1 3UP Durham, United Kingdom; [47]Sapienza University and ICRA, p.le A. Moro, 2 - 00185, Rome, Italy; [48]University of Iowa, Van Allen Hall, Iowa City, IA 52242, United States; [49]Michigan state University, 567 Wilson Rd, - MI 48824 East Lansing, United States; [50]Copernicus Astronomical Center, Bartycka 18 - Warsaw, Poland; [51]George Washington University, 2121 I St NW, Washington, DC 20052, United States; [52]Cornell University, Space Building - NY 14853 Ithaca, United States; [53] University of Illinois, Physics Department, 1110 W. Green St., Urbana, IL 61801, United States; [54]Dipartimento di Fisica, Università degli Studi di Milano, Via Celoria 16, 20133 Milano, Italy; [55]University of Trieste, Via Alfonso Valerio, 32 - 34128 Trieste, Italy; [56]Pavia University, Corso Strada Nuova, 65 - 27100 Pavia, Italy; [57]INAF IASF, Via Ugo La Malfa, 153 - 90146 Palermo, Italy; [58]University of California, Santa Cruz, 1156 High St. CA 95064 Santa Cruz, United States; [59]University of Rome III, Via della Vasca Navale, 84 - 00146 Roma, Italy; [60]University of Melbourne, Swanston Street - VIC 3052 Parkville, Australia; [61]Kapteyn Astronomical Institute, University of Groningen, P.O. Box 800, 9700 AV Groningen, The Netherlands; [62]University of Maryland, Department of Astronomy, College Park, MD 20742-2421, United States; [63]National Institute of Aerospace Technology (INTA), Carretera de Ajalvir km. 4 - 28850 Torrejón de Ardoz, Spain; [64]University of Alberta, 85 Avenue 116 St NW - AB T6G 2R3 Edmonton, Canada; [65]Observatoire Astronomique de Strasbourg, 11 rue de l'Université - 67000

Strasbourg, France; [66]Université Paris Diderot 5 rue Thomas-Mann 75205 Paris cedex 13, France; [67]INAF-OA Torino, Via Osservatorio, 20 - 10025 Pino Torinese, Italy; [68]Space Research Centre, Warsaw, Bartycka 18A - Warszawa, Poland; [69]Space Telescope Institute, 3700 San Martin Drive - MD 21218 Baltimore, United States; [70]University of Arizona, Department of Astronomy, 933 N. Cherry Ave, Tucson, AZ 85721, United States; [71]Raman Research Institute, C. V. Raman Avenue - 560 080 Sadashivanagar, India; [72]Czech Technical University in Prague, Zikova 1903/4, CZ-166 36 Praha 6, Czech Republic; [73]Tuorla Observatory, University of Turku, Väisäläntie 20, FIN-21500 Piikkiö, Finland; [76]Armagh Observatory, College Hill - BT61 9DG Armagh, United Kingdom; [77]INFN, Trieste, Via A. Valerio 2 - I-34127 Trieste, Italy; [78]NRL, 4555 Overlook Ave. SW Washington, DC 20375-5352, United States; [80]Institute for Nuclear Theory, University of Washington, WA 98195-1550 - Seattle, United States; [81]Physics Department, University of Crete, GR-710 03 Heraklion, Greece; [82]Instituto de Astrofisica de Canarias, Vía Láctea s/n, La Laguna, E-38205, Tenerife, Spain; [83]Leiden Observatory, Niels Bohrweg 2 - NL-2333 CA Leiden, The Netherlands; [84]KTH Royal Institute of Technology, Valhallavägen 79 - 100 44 Stockholm, Sweden; [85]INAF-IASF-Milano, Via E. Bassini 15 - I-20133 Milano, Italy; [86]Silesian University in Opava, Na Rybníčku 626/1 - 746 01 Opava, Czech Republic; [87]University of Erlangen-Nuremberg, Schlossplatz 4 - 91054 Erlangen, Germany; [88]ExtreMe Matter Institute EMMI, GSI Helmholtzzentrum für Schwerionenforschung GmbH, 64291 Darmstadt; [89]Leibniz-Institut fuer Astrophysik Potsdam, An der Sternwarte 16 - 14482 Potsdam, Germany; [90]National University of Ireland Galway, University Road, Galway, Ireland; [91]University of Manchester, Booth Street West - M15 6PB Manchester, United Kingdom; [92]Aristotle University of Thessaloniki, Greece; [93]Goddard Space Flight Center, 8800 Greenbelt Rd. - Md., 20771 Greenbelt, United States; [94]ISAS, 3-1-1 Yoshinodai, Chuo-ku, Sagamihara - 252-5210 Kanagawa, Japan; [95]University of Alicante, Carretera San Vicente del Raspeig - 03690 Sant Vicent del Raspeig, Spain; [96]ICREA - Institució Catalana de Recerca i Estudis Avançats, Passeig Lluís Companys, 23 - 08010 Barcelona, Spain; [97]Physical Institute of the Academy of Sciences of the Czech Republic, Na Slovance 1999/2, CZ-182 21 Praha 8, Czech Republic; [98]University of Warwick, Gibbet Hill Road - CV4 7AL Coventry, United Kingdom; [99]INAF-OA Padova, Vicolo Osservatorio 5, Padova, Italy; [100]University of Nevada, Las Vegas, NV 89012, United States; [101]University of Rome Tor Vergata, Via della Ricerca Scientifica 1 - 00133 Rome, Italy; [102]INAF-IRA-Bologna, Via P. Gobetti 101- 40129 Bologna, Italy; [103]University of Bologna, Dept. of Physics and INFN section of Bologna, V.le Berti Pichat, 6/2, 40127, Bologna, Italy; [104]Departamento de Astrofisica, Universidad de La Laguna, La Laguna, E-38206, Santa Cruz de Tenerife, Spain; [105]APC, AstroParticule & Cosmologie, UMR 7164 CNRS/N2P3, Université Paris Diderot, CEA/Irfu, Observatoire de Paris, Sorbonne Paris Cite 10 rue Alice Domon et Leonie Duquet, 75205 Paris Cedex 13, France; [106]INAF- Osservatorio Astronomico di Palermo, Piazza del Parlamento 1, 90134 Palermo, Italy; [107]School of Physics and Astronomy, University of Southampton, Southampton, SO17 1BJ, UK; [108]Kepler Institute of Astronomy, University of Zielona Gòra, Lubuska 2, 65-265, Zielona Gòra, Poland; [109]University of California, San Diego, Mail Code 0424, La Jolla, CA 92093 United States; [110]Dept. of Astronomy, Univ. of Wisconsin, 475 N. Charter Str., Madison WI 53706, United States; [111]Wayne State University, Department of Physics & Astronomy, 666 W. Hancock St, Detroit, MI 48201, United States; [112]Centro de Astrobiologia (CSIC--INTA), P.O. Box 78, E-28691, Villanueva de la Cañada, Madrid, Spain; [113]Foundation for Research and Technology - Hellas, GR-711 10 Heraklion, Greece; [114]CNES, 18 Avenue Edouard Belin, 31400 Toulouse, France; [115]INAF-OA Cagliari, località Poggio dei Pini, Strada 54, 09012 Capoterra, Italy; [116]Instituto Astrofisica de Andalucia, Glorieta de la Astronomía (IAAC-CSIC),

s/n., E-18008, Granada, Spain; [117]University of Pisa, Largo B. Pontecorvo 3, Pisa, I-56127 Italy; [118]Perimeter Institute for Theoretical Physics, 31 Caroline Street North, Waterloo, ON, N2L 2Y5, Canada; [119]Dipartimento di Scienze Fisiche, Università di Napoli Fedelico II, C.U. di Monte Sant'Angelo, Via Cintia ed. 6, 80126, Napoli, Italy; [120]School of Physics and Astronomy, University of Birmingham, Edgbaston B15 2TT, Birmingham, United Kingdom; [121]University of California, Berkeley, Space Sciences Laboratory, 7 Gauss Way, Berkeley, CA 94720-7450; [122]Ohio University, Department of Physics & Astronomy, Athens, OH 45701, United States; [123]Max-Planck-Institut fuer extraterrestrische Physik, Postfach 1603, 85740 Garching, Germany; [124]Max Planck Institute for Gravitational Physics (Albert Einstein Institute), Am Mühlenberg 1, D-14476 Golm, Germany; [125]University of Valencia, Av de Vicente Blasco Ibáñez, 13, 46010 Valencia, Spain; [126]Technical University of Catalonia, C. Jordi Girona, 31, 08034 Barcelona, Spain; [127]Department of Physics and Astronomy, University of Waterloo, 200 University Avenue West, Waterloo, ON, N2L 3G1, Canada; ; [128]Sapienza University, p.le A. Moro, 2 - 00185, Rome, Italy; [129]Argelander-Institut für Astronomie, Auf dem Hügel 71, D-53121, Bonn, Germany; [131]Texas Tech University, Physics Department, Box 41051, Lubbock, TX 79409-1051; [132]Tata Institute of Fundamental Research, 1 Homi Bhabha Road, Colaba, Mumbai 400005, India; [133]Charles University in Prague, Faculty of Mathematics and Physics, V Holesovickach 2, CZ18000 Prague, Czech Republic; [134]Jorgen Sandberg Consulting, Denmark; [135]Istanbul Kültür University, Faculty of Science and Letters, Ataköy Campus, Bakırköy 34156, Istanbul, Turkey; [136]Fundamental Physics Department, Facultad de Ciencias-Trilingüe University of Salamanca, Plaza de la Merced s/n, E-37008 Salamanca, Spain; [137]Departamento de Física Atómica, Molecular y Nuclear, Facultad de Ciencias, Universidad de Granada, E-18071-Granada-Spain; [138]University of Surrey, Guildford, Surrey GU2 7XH, United Kingdom; [139] Washington University, Dept. of Physics- Compton Hall, One Brookings Drive - Campus Box 1105, St. Louis, MO 63130, United States; [140]Oxford University, Department of Physics, Clarendon Laboratory, Parks Road, Oxford, OX1 3PU, United Kingdom; [141]ASTRON, the Netherlands Institute for Radio Astronomy, Postbus 2, 7990 AA Dwingeloo, The Netherlands; [142]Department of Astronomy and Astrophysics, The Pennsylvania State University, 525 Davey Lab, University Park, PA 16802, USA; [143]Institute of High Energy Physics, 19B YuquanLu, Shijingshan district, Beijing, 1000049, China; [144]Shanghai Astronomical Observatory, 80 Nandan Road, Shanghai 200030, China; [145]Department of Engineering Physics and Center for Astrophysics, Tsinghua University, Beijing 100084, China; [146]Tongji University, Institute of Precision Optical Engineering, Department of Physics, Shanghai 200092, China; [147]National Astronomical Observatories, Chinese Academy of Sciences, 20A Datun Road, Chaoyang District, Beijing, China; [148]Nanjing University, 22 Hankou Road Nanjing Jiangsu 210093 P.R.China; [149]Purdue University, 525 Northwestern Avenue, West Lafayette, IN 47907, United States; [150]Shanghai Academy of Spaceflight Technology, Yangpu City Industrial Park,No.135, Guowei Road,Yangpu District, Shanghai, China; [151]China Academy of Space Technology, Haidian District, Beijing, China; [152]University of Science and Technology of China, No.96, JinZhai Road Baohe District,Hefei,Anhui, 230026, China; [153]Peking University, No.5 Yiheyuan Road Haidian District, 100871, Beijing, China; [154]Guangxi University 188, East Daxue Road Nanning, Guangxi 530006, China; [155]Purple Mountain Observatory, CAS,2 West Beijing Road, Nanjing 210008, China; [156]Department of Physics, University of Basel,, Klingelbergstr. 82, 4056 Basel, Switzerland; [157]LUTH, Univ. Paris Diderot, 5, place Jules Janssen, 92195 Meudon, France; [158]IPN Lyon, 4, Rue Enrico Fermi, 69622, Villeurbanne Cedex, Lyon, France; [159]CERN, Switzerland ; [160]Scuola Normale Superiore di Pisa, Piazza dei Cavalieri, 7, 56126 Pisa, Italy; [161]NYUAD, PO Box 129188., Abu Dhabi, United Arab Emirates;

[162]Georgia Institute of Technology, North Ave NW, Atlanta, GA 30332, United States; [164]Joint Institute for VLBI in Europe (JIVE), Postbus 2, 7990 AA Dwingeloo, The Netherlands; [165]Max-Planck-Institut für Radioastronomie, Auf dem Hügel 69, D-53121 Bonn (Endenich), Postfach 20 24, D-53010 Bonn; [167]Department of Mathematics and Physics, University of Salento, and INFN, via per Arnesano, CP 193, 73100, Lecce, Italy; [168]Radboud Universiteit Nijmegen, Comeniuslaan 4, 6525 HP Nijmegen, The Netherlands; [169]Astrophysics Research Institute, Liverpool John Moores University, IC2, Liverpool Science Park, 146 Brownlow Hill, Liverpool L3 5RF, United Kingdom; [170]JILA, University of Colorado, 440 UCB, Boulder, CO 80309; [171]IUSS - Istituto Universitario di Studi Superiori di Pavia, Palazzo del Broletto - Piazza della Vittoria n.15, 27100 Pavia (Italia); [172]University of Zielona Gora, 65-417 Zielona Góra, Poland; [173]Department of Physics, University of Perugia, I-06123 Perugia, Italy; [174]INAF-IFSI Torino, corso Fiume 4, 10133 Torino, Italy; [175]Los Alamos National Laboratory, Los Alamos, NM 87545, United States; [176]Columbia University, 116th St & Broadway, New York, NY 10027, United States; [177]RIKEN, Japan; [178]Dept. of Physics and Astronomy, Stony Brook University, Stony Brook, NY 11794-3800, United States; [179]Sternberg Astronomical Institute, Moscow M.V. Lomonosov State University, 119992 Moscow, Russia; [180]University of Baskent, Department of Electrical and Electronic Engineering, Ankara, Turkey; [181]Technion - Israel Institute of Technology, Technion City, Haifa 3200003, Israel; [182]Harvard-Smithsonian Center for Astrophysics, 60 Garden Street, MA 02138 Cambridge, USA; [183]CRESST and X-ray Astrophysics Laboratory, NASA/GSFC, Greenbelt, MD 20771, United States; [184]University of Vienna, Department of Astrophysics, Türkenschanzstrasse 17, A-1180 Vienna, Austria; [185]Università degli Studi di Urbino Carlo Bo, Piazza della Repubblica 13, I-61029, Urbino, Italy; [186]University of Alabama in Huntsville, 301 Sparkman Drive, Huntsville, Alabama, USA; [187]Dipartimento di Fisica, Universita' di Trento, via Sommarive, 14, I-38123, Trento Italy; [188]INFN, Via Santa Sofia, 64, 95123 Catania, Italy; [189]Institut für Theoretische Physik, Goethe Universität, D-60438 Frankfurt am Main, Germany; [190]GSI Helmholtzzentrum für Schwerionenforschung GmbH, Planckstrasse 1, 64291 Darmstadt, Germany; [191]Institut für Kernphysik, Technische Universität Darmstadt, 64289 Darmstadt, Germany; [192]Institute of Astronomy and Astrophysics Université Libre de Bruxelles, CP 226, Boulevard du Triomphe, B-1050 Brussels, Belgium ; [193]Department of Physics and Mathematics, Aoyama Gakuin University, Sagamihara-shi Kanagawa 252-5258, Japan; [194]National Space Science & Technology Center, University of Alabama in Huntsville, Huntsville, AL 35805, United States; [195]Department of Physics, Tohoku University, Aramaki, Aoba-ku, Sendai 980-8578, Japan; [196]Institute of Astronomy, University of Cambridge, Madingley Road, Cambridge, CB3 0HA, United Kingdom; [197]School of Physical Sciences, Dublin City University, Glasnevin, Dublin 9, Ireland; [198]Laboratory of Physics and Chemistry of the Environment and Space (LPC2E), University of Orleans, CNRS, France; [199]Centre for Space, Atmospheric and Oceanic Science, Department of Electronic and Electrical Engineering, University of Bath, Bath, UK; [200]China Academy of Space Technology, China; [201]Instituto de Ciencias Nucleares, UNAM, Apartado Postal 70-543, Ciudad Universitaria, Mexico D.F. 04510, Mexico; [202]Department of Astronomy, The Ohio State University, 4055 McPherson Laboratory, 140 West 18th Avenue, Columbus, OH 43210-1173, United States; [203]Center for Data Science, New York University, 726 Broadway, 7th Floor, New York, NY 10003, United States; [204]University of Tennessee, Knoxville, TN 37996, United States; [205]Fondazione Bruno Kessler, via Sommarive, 18, I-38123, Trento Italy; [206]Trento Institute for Fundamental Physics and Applications, via Sommarive, 14, I-38123, Trento Italy

ABSTRACT

The Large Observatory For x-ray Timing (LOFT) is a mission concept which was proposed to ESA as M3 and M4 candidate in the framework of the Cosmic Vision 2015-2025 program. Thanks to the unprecedented combination of effective area and spectral resolution of its main instrument and the uniquely large field of view of its wide field monitor, LOFT will be able to study the behaviour of matter in extreme conditions such as the strong gravitational field in the innermost regions close to black holes and neutron stars and the supra-nuclear densities in the interiors of neutron stars. The science payload is based on a Large Area Detector (LAD, >8m^2 effective area, 2-30 keV, 240 eV spectral resolution, 1 degree collimated field of view) and a Wide Field Monitor (WFM, 2-50 keV, 4 steradian field of view, 1 arcmin source location accuracy, 300 eV spectral resolution). The WFM is equipped with an on-board system for bright events (e.g., GRB) localization. The trigger time and position of these events are broadcast to the ground within 30 s from discovery. In this paper we present the current technical and programmatic status of the mission.

Keywords: X-ray astronomy, Silicon detectors, timing, spectroscopy

1. INTRODUCTION

The Large Observatory For x-ray Timing (LOFT) is a mission concept originally proposed to ESA under the Cosmic Vision call M3 for the study of matter under extreme conditions of density (equation of state of matter at supra-nuclear density) and gravity (test of General Relativity in strong-field regime). LOFT was selected in 2011 as M3 mission candidate and performed a Phase 0/A study within the ESA context until 2013. Under the coordination and responsibility of ESA, a Consortium of institutes in the ESA member states studied the scientific payload and science ground segment, the Astrium-D and Thales Alenia Space-I companies performed competitive system studies of the spacecraft and system, while ESA led the study of the ground segment and operations. LOFT was eventually not selected as M3 mission in the final competition in early 2014. The main results of the ESA LOFT-M3 study are reported in a set of publicly available ESA documents, namely the Yellow Book [1], the Science Requirements Document [2], the Payload Definition Document [3], the Mission Requirements Document [4] and the Preliminary Requirements Review Technical and Programmatic Report [5]. Additional information may be found in [6, 7, 8, 9] and references therein. Despite the eventual non-selection as M3 mission, the science proposed with LOFT was highly ranked during the review process and the ESA PRR panel assessed the mission technical and programmatic feasibility within the budget and the schedule imposed by the M3 ESA planning, at low risk [5].

In 2014 ESA issued a new mission call, M4, with boundary conditions tighter than the previous call. The ESA budget (cost at completion) was reduced to 450 M€ (as compared to the 550 M€ final budget of M3) and a slightly faster development schedule was requested. The new M4 conditions thus required a revision of the LOFT-M3 configuration, especially to comply with the reduced budget. The sensitivity analysis carried out during the M3 study (see [2]) showed that the LOFT-M3 design was over-performing with respect to its scientific objectives and this allowed to revise the size of the LAD and the WFM instruments for M4, with essentially no loss in science. This choice led also to a significant reduction in the payload and system costs, while improving the development schedule, matching the M4 requirements with significant margins. In contrast to the M3 mission opportunity, M4 was better open to international collaborations. International partners participating to the LOFT-M3 science could eventually join and commit to contribute to the mission development as well. In particular, CNSA and CAS (China National Space Administration and Chinese Academy of Sciences) committed to provide the deployment system (tower, panels and mechanisms) and the VHF transmission system, ISAS and the University of Tohoku committed to the development and provision of the LAD collimators (as manufactured by Hamamatsu), while ISRO (Indian Space Research Organization) committed to provide an additional ground station to expand the telemetry transmission capabilities, with a significant benefit in the science output of the mission (especially with the WFM). The international participation enabled additional cost savings on the ESA budget, making the LOFT-M4 proposal better compliant with the M4 budget requirements, still at no cost in science.

In this paper we mostly focus on the changes implemented in the LOFT-M4 proposal with respect to the M3 configuration, referring the reader to the references cited above for an extensive description of the baseline LOFT science and configuration, as developed during the M3 study.

2. SCIENCE DRIVERS

LOFT addresses the Cosmic Vision theme "Matter under extreme conditions" by probing the properties of the densest matter and the strongest gravitational fields in our Universe to unprecedented degree. It will revolutionize these fundamental areas by X-ray observations of accreting neutron stars (NS) and black holes (BH) across the mass scale. The matter inside NS and the space-time close to BH are among the uncharted territories of fundamental physics: accreting NS and BH provide a unique arena for the exploring these. The fundamental diagnostic of dense-matter interactions is the equation of state (EOS), the pressure-density temperature relation of matter. This is observationally encoded as the NS mass-radius (M-R) relation. The EOS is set by as yet unverified aspects of the strong force that theory alone cannot address, such as the possible emergence, at the highest densities, of deconfined quarks and/or strange matter. Experiments and observations are essential to drive progress. LOFT's very large effective area up to 30 keV will permit the first precise MR measurements for a range of NS of different mass. The use of complementary methods (profile modelling of 3 types of pulsations, maximum spin rates, seismology) makes LOFT unique in its ability to overcome systematics. The measured M-R relation will allow direct reconstruction of the EOS of cold supranuclear-density matter. General Relativity (GR), verified to exquisite accuracies by precisely measuring small effects in weak fields (e.g., binary millisecond radio pulsars), predicts large effects, as yet unverified, in the motions of matter and photons in strong-field gravity. These include frame dragging, extreme light bending, and extreme orbital motion effects very close to BH. LOFT will measure such effects down to a few Schwarzschild radii with several complementary methods simultaneously. Dynamical time-scale variations in relativistic iron lines will be precisely quantified using CCD-class spectral resolution spectra and enormous, pileup-free throughput. Timing features such as high-frequency quasi-periodic oscillations (QPOs) will verify key predictions of strong-field GR.
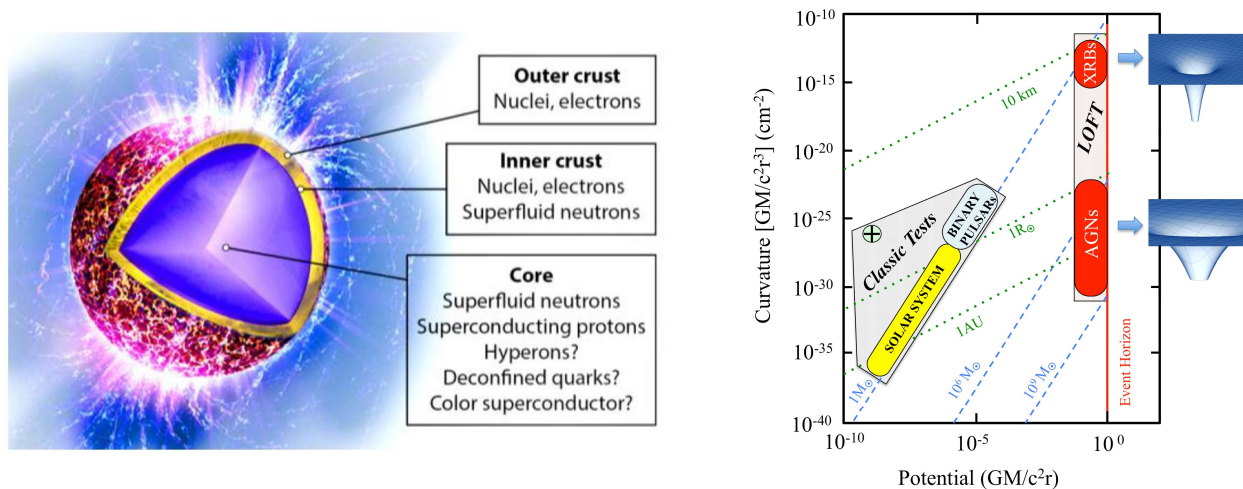
Figure 1. Left: Schematic structure of a neutron star. The outer layer is a solid ionic crust supported by electron degeneracy pressure. Neutrons begin to leak out of ions (nuclei) at densities $\sim 4 \times 10^{11}$ g/cm^3 (the neutron drip line, which separates inner from outer crust), where neutron degeneracy also starts to play a role. At densities $\sim 2 \times 10^{14}$ g/cm^3, the nuclei dissolve completely. This marks the crust-core boundary. In the core, densities may reach up to ten times the nuclear saturation density of 2.8×10^{14} g/cm^3 (the density in normal atomic nuclei). (Graphics credit: NASA). Right: LOFT probes the deepest gravitational wells in the Universe: BHs. Current GR tests use potentials 10^4 times lower. LOFT uniquely covers a factor 10^{16} in spacetime curvature with uniform diagnostics.

2.1 Dense Matter

Neutron stars access a unique regime of parameter space at high density and low temperature. Densities in NS cores can reach ~ 10 times the density of an atomic nucleus, forming states of matter that cannot exist in the laboratory. The low temperatures permit the formation of nuclear superfluids, and the long lifetimes of NS permit long timescale weak interactions to reach equilibrium. This generates matter that is neutron-rich and which may contain deconfined quarks or particles with non-zero net strangeness. Connecting NS observables to strong interaction physics can be done because the forces between the nuclear particles set the stiffness of neutron star matter. This is encoded in the Equation of State. The EOS in turn sets the NS mass M and radius R via the stellar structure equations. By measuring and then inverting the

M-R relation, we can recover the EOS (Figure 2). Measuring the EOS of supranuclear density matter is of major importance to both fundamental physics and astrophysics. It is central to understanding NS, supernovae, and compact object mergers involving at least one NS (prime gravitational wave sources and the likely engines of short gamma-ray bursts). To distinguish the models shown in Figure 2, one needs to measure M and R to precisions of a few %, for several masses. To date, most efforts to measure the M-R relation have come from modeling the spectra of thermonuclear X-ray bursts and quiescent low-mass X-ray binaries. The constraints obtained so far are weak. The technique also suffers from systematic errors of at least 10% due to several effects. Constraints have also come from radio pulsar timing, where the masses of NS in compact binaries can be measured very precisely: high mass stars give the strongest constraint. However even the discovery of pulsars with masses ≈2$M_\odot$, has left a broad range of EOS viable (Figure 2).

LOFT will employ three primary techniques to measure M and R: pulse profile modeling, spin measurements and seismology. These involve different types of NS: accreting NS with thermonuclear bursts, accretion powered X-ray pulsars, and isolated highly magnetic NS known as magnetars. The use of multiple techniques and different source types permits independent cross-checks on the EOS. An extensive discussion of the dense matter science case and state of the art and an analysis of the methods proposed by LOFT to address them may be found in [2] and [10].
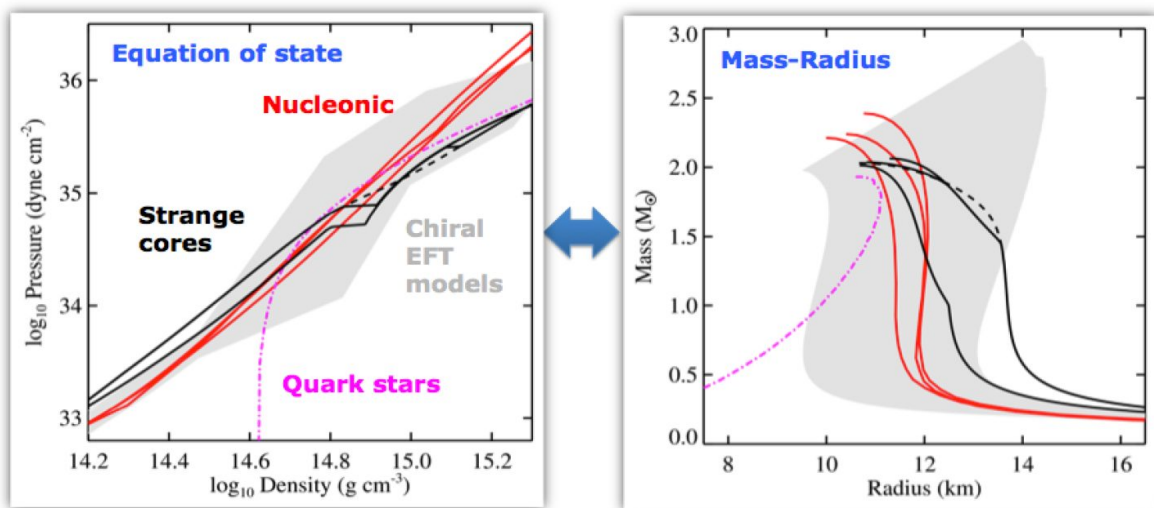

Figure 2. The pressure density relation (EOS, left) and the corresponding M-R relation (right) for some example models with different microphysics. Grey band: range of nucleonic EOS based on chiral effective field theory. Red: nucleonic EOS. Black solid: Hybrid models (strange quark core. Black dashed: Hyperon core models. Magenta: A quark star model. Adapted from [10].

2.2 Strong Field Gravity

LOFT will use time-resolved spectroscopy to directly measure the motions of matter in the intense gravity near the event horizons of accreting black holes. This will test the effects of strong-field gravity to an unprecedented degree. Where the traditional best tests of General Relativity (GR) use millisecond radio pulsars orbiting in gravitational fields similar to those in our Solar System, and therefore rely on small effects, LOFT probes gravitational fields that are truly strong, where Einstein's theory predicts gross deviations from Newtonian physics. LOFT will measure these large GR effects at few-percent precision, and test alternative theories of gravity. LOFT will directly compare the dynamics near stellar-mass and supermassive black holes (BH), covering a factor 10^8 in mass and 10^{16} in space-time curvature (Figure 1). Comparative studies of neutron stars will directly test for uniqueness of BH phenomena. The transformative nature of LOFT's strong field gravity studies comes from merging, for the first time, the two powerful, but so far separate, diagnostics we have of the strong-gravity regions: fast X-ray timing and X-ray spectroscopy. Because of its much larger effective area in the Fe-K region, LOFT measures fluctuations and resolves relativistic iron lines at up to several hundred times the photon throughput of other designs. This provides the capability to measure rapid variability in narrow bands within the broad iron line profile. On the brightest black holes LOFT attains signal to noise levels to rapid iron line variability more than a hundred times those of currently operating or planned missions. So, crucially, LOFT sees fluxes

and line profiles vary on the fundamental strong-field relativistic timescales, resolving motions down to very close to the event horizon and hence to understand how matter moves in strong-field gravity.

LOFT is part of a much broader effort to understand gravity in the strong-field regime, which is a cutting-edge issue in current (astro)physics. Several complementary approaches to this goal, all challenging, are currently being pursued. Gravitational waves occur when spacetime is being violently shaken and hence dynamic. LOFT, in contrast, addresses stationary spacetimes: it probes black holes by observing hot plasma orbiting them. Essentially, the plasma serves as a luminous test fluid. Other (near-)stationary spacetime approaches, such as extreme mass-ratio binary orbital dynamics and sub-mm imaging of nearby weakly accreting AGN to detect the BH shadow are limited to supermassive BH. LOFT uniquely covers not only supermassive but also stellar-mass black holes with uniform, well-established diagnostics. At given potential, GR orbits simply scale with mass, and are independent of spacetime curvature; this does not generally hold in alternative theories of gravity. However, only near stellar-mass compact objects do spacetime curvatures occur much in excess to those in the Solar System. Hence, only LOFT can test this, and it will do so over 16 decades in curvature (Figure 1).

Relativistic iron lines and variability on relativistic time scales, in particular, quasi-periodic oscillations (QPOs) are well-established diagnostics providing detailed insight into BH accretion flows. Fe-Kα lines are successfully modeled by 'reflection' of hard continuum radiation by the relativistic BH disk. They directly probe orbital radii and velocities, gravitational potentials and photon geodesics, and yield estimates of BH spins. Partially ionized absorption plays a role and is included in our simulations. Rapid variability is caused by plasma motion in the inner flow. QPOs are observed at frequencies within 10-20% of the GR-predicted 'fundamental' frequencies of the relativistic orbital, epicyclic and precessional motions. The highest observed frequencies are close to the high frequencies that GR predicts to occur at the innermost stable circular orbit (ISCO), and they scale with M^{-1} as predicted. Models involve near-geodesically orbiting density fluctuations and global disk oscillation- and precession-modes. There is large progress in first-principle MHD calculations; some begin to show the observed QPOs.

LOFT focuses on BH, with comparative studies of NS. Neutron-star QPO frequencies also likely derive from fundamental frequencies and NS spins, measured directly, calibrate the frame dragging effects that in BH we use to measure spin (Figure 3). However, the absence of stellar magnetic and radiative stresses makes black holes the clean environment gravity studies need. BH orbital frequency QPOs are weak, transient and at the edge of current capabilities, but in one observation the three GR-predicted fundamental frequencies were observed. Alternative explanations for QPOs have been discussed, but do not predict the correlated variable QPO frequencies as successfully as relativistic models. Rapid Fe line variability is key, and that it exists shows the line is formed in the strong gravity regions [11]. However, so far energy resolution and/or signal to noise were much too low to draw conclusions from this variability about strong gravity. Lines and variability both arise in the hot, turbulent plasma flows in the strong-field region, and provide complementary diagnostics (spectroscopy: velocities and redshifts; timing: fundamental frequencies). Merging these with LOFT gives qualitatively new types of information and probes the strong-field regions to an unprecedented degree. A deeper and more extensive discussion of the LOFT science case on strong field gravity may be found in [1] and [11].
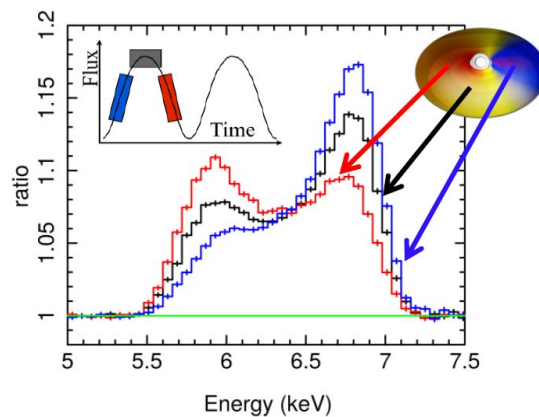

Figure 3. Changes in the iron line profile due to relativistic frame-dragging induced precession of the accretion flow around a Kerr black hole. LOFT measures the repetitive line distortions to high precision.

2.3 Observatory science

With a uniquely high throughput, good spectral resolution and wide sky coverage, LOFT is an observatory very well suited for a variety of studies complementing the core science of sources down to less than 0.01 mCrab. The LAD will provide the best timing and spectroscopic studies ever for a wide range of high energy sources brighter than ~1 mCrab in the 2-30 keV band. The WFM, with its unprecedented combination of field of view and imaging, makes LOFT a discovery machine of the variable and X-ray transient sky, which will reveal many new sources for follow-up with the LAD and other facilities. As previous missions have shown, newly discovered, unforeseen types of sources will then provide unexpected insights into fundamental questions. The WFM will also be monitoring daily hundreds of sources, to catch unexpected events and provide long-term records of their variability and spectroscopic evolution. LOFT is also a unique, powerful X-ray partner of other new large-scale facilities across the spectrum likely available in the 2020s, such as advanced gravitational wave and neutrino experiments, SKA and pathfinders in the radio, LSST and E-ELT in the optical, and CTA at TeV energies (Figure 4). Some key targets of the observatory science program (e.g., low-mass X-ray binaries, magnetars) will be observed in LOFT's core program as well. Some observatory science goals can actually be pursued from these same observations. Other targets of the observatory science program (e.g., accreting white dwarfs, blazars, high mass X-ray binaries), can in turn provide useful comparative insights for the core science objectives as well. To explain fully the science case for LOFT as an observatory, more than 300 scientists from the community at large have published 12 White Papers [12-23] addressing several aspects of the astrophysics on which LOFT will enable significant advances, e.g.: accretion and ejection in X-ray binaries, pulsar magnetospheric physics, thermonuclear X-ray bursts, high mass X-ray binaries and ultraluminous X-ray sources, gamma ray bursts, tidal disruption events, blazars, radio-quiet AGNs, cataclysmic variables, binary evolution, flare stars and the terrestrial physics of gamma ray flashes.
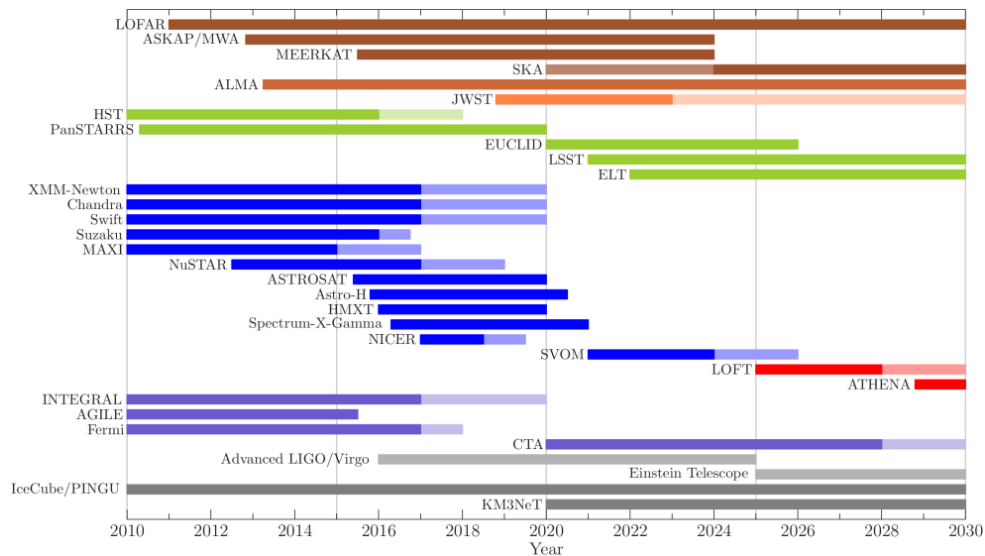
Figure 4. Multiwavelength and GW facilities relevant to LOFT. Colors indicate similar wavebands from the radio (top) via IR and optical to X-rays and gamma rays. Grey bands: gravitational wave and neutrino detectors. Dark colors: current end of funding, light colors: expected lifetime, where known, independent of funding decisions. Missions might last longer.

3. THE LOFT-M4 CONFIGURATION

3.1 Mission configuration and profile

The proposed LOFT mission for the M4 flight opportunity adopts the same 5-panel design identified by the M3 ESA study carried out by Thales Alenia Space and endorsed by the PRR Panel [5], simplified by a 20% reduction in the LAD geometric area and number of WFM cameras. Also the work-share between ESA and the LOFT Consortium is simplified by shifting the PLM responsibility entirely to the Consortium. Figure 5 provides an overview of the mission architecture.

LOFT will be placed in to an equatorial Low Earth Orbit (LEO), with an inclination <2.5° and altitude 550 km. This orbit has been selected to minimise the radiation dose (and subsequent NIEL damage) to the SDDs, allowing them to be

operated at temperatures which are compatible with passive thermal control (-10°C at the end of the nominal mission for the LAD), while maintaining the required energy resolution performance of the instruments (the LAD energy resolution being the most driving requirement). This orbit provides near-complete shielding of the Spacecraft (SC) by the geomagnetic field against solar particle events and cosmic rays – damage to the SDDs is then dominated by contributions from trapped proton populations due to the van Allen belts and charge-exchange soft protons. The low altitude and inclination serve to minimise the trapped charged particles in the van Allen belts as seen by the SC, avoiding especially the South Atlantic Anomaly.
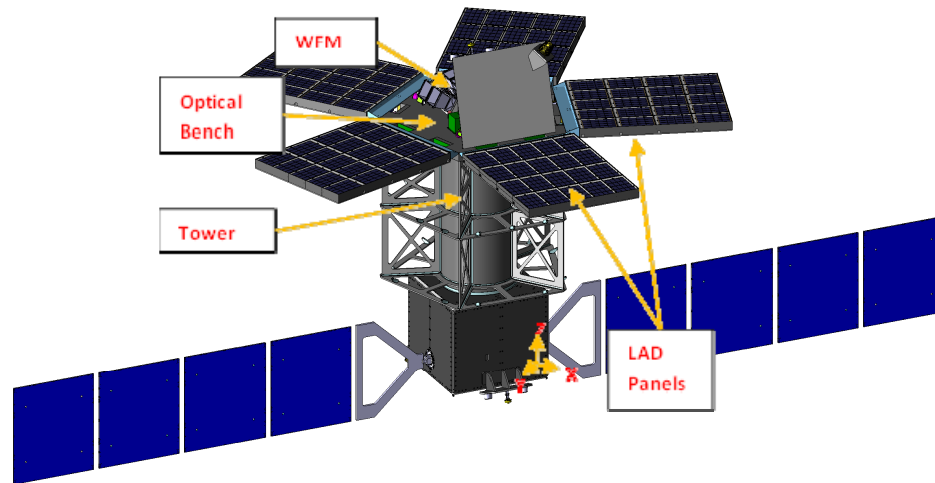

Figure 5. The TAS-I concept of the payload module tower with the optical bench and the 5 deployed panels adopted for the LOFT-M4 baseline design

The performance of the Soyuz-Fregat launch vehicle (from Kourou) to the chosen orbit is considerable (over 6000 kg, taking into account ESA margin policy of 5% reduction in predicted launcher capability). Against this, the spacecraft design has very large mass margins. The total launch mass was estimated as 3600 kg, including all margins, the propellant and the launch adapter. This provides a >2 tons of spare launcher capability.

The key aspects of design of the LOFT SC are driven by the accommodation of the LAD (12 m^2 of geometric area, 100 LAD Modules), its operating temperature and thermal stability, and pointing and availability requirements (1 arcmin class, effective area stability requirements expressed as percentages in the frequency domain [2]). The SC is divided into a Payload and a Service Module (PLM and SVM). Clearly the SC is dominated by the LAD panels, which by necessity are deployable in order to achieve the accommodation of the required number of modules. The accommodation of the folded spacecraft in its 5-panel configuration in the Soyuz-Fregat fairing was demonstrated during the M3 study. The reduced LAD area further reduces the spacecraft height by 63 cm, improving the compatibility even further. The WFM is housed on top of the PLM (such that the centre of its response is aligned with the LAD bore-sight) on a platform, the Optical Bench, whose plane is parallel with the nominal sun direction, and located behind a dedicated sun shield. The Optical Bench comprises the structural supports for the LAD and WFM and Instrument Control Units, Star Trackers (to minimise AOCS reference frame distortion with respect to instruments), a Payload Data Handling Unit (PDHU), which provides services such as mass memory, science data and burst data management, control of payload heaters and distribution of PPS time signals, and interface to the SC On Board Data Handling (OBDH).

3.2 Large Area Detector (LAD)

The LAD instrument proposed for the M4 call has the same design as studied for M3 (e.g., [8]), with a slight downscale in area size. The 5-panel LOFT-M3 design offered ~9.8 m^2 effective area performance, the proposed 5-panel design for M4 envisages a 20% smaller LAD geometric area, yet providing ~8.5 m^2 effective area, owing to the higher open area of the new collimator (see below). The measurement principle of the LAD is the photon-by-photon observation of X-ray sources in the nominal energy range 2-30 keV (up to 80 keV in expanded mode, for out-of-field-of-view burst events).

The measurement by silicon detectors of the time and energy characteristics of the individual source photons, both at high resolution and with enormous statistics, enables unprecedented spectral-timing studies, as discussed in the previous sections. The field of view is limited to ~1° by a mechanical collimator to reduce source confusion and the X-ray background. The key instrument requirements and anticipated performance are listed in Table 1. We note that all M3 requirements and anticipated performance are confirmed, with the exception of the effective area, as discussed above, and the anticipated background, improved thanks to a larger stopping power of the new collimator.

The LAD large area is achieved by a modular and intrinsically highly redundant design based on LAD Modules. Each Module consists of a set of 4 x 4 detectors and 4 x 4 collimators, supported by two grid-like frames. The Module also hosts the read-out electronics, as well as the power supplies, organized in the Front-End Electronics (FEE) and Module Back-End Electronics (MBEE). The LAD Modules are organized in large Panels, deployable from an optical bench supported by a central tower. Each of the 5 LAD Panels hosts 20 (5x4) Modules, for a total of 100 Modules or 1600 detectors, and a Panel Back-End Electronics (PBEE), in charge of interfacing the 20 Modules to the central Instrument Control Unit (ICU). Realizing such a large detector within the budgets of an M-class mission became feasible thanks to recent developments in detector technology. Large-area Silicon Drift Detectors (SDDs) were developed for the ALICE/LHC experiment at CERN and later optimized for the detection of photons to be used on LOFT, with typical size of 11 x 7 cm^2 and 450 μm thickness (e.g, [24]). Each detector is segmented in two halves with 112 channels each (970 μm pitch anodes). Despite detecting as many as ~200 000 counts per second from the Crab, the segmentation into 1600 detectors and ~360 000 electronics channels means that the rate on the individual channel is very low even for very bright sources, removing any pile-up or dead-time issues. To maintain a good energy resolution at the end of life, the detectors need to be moderately cooled (-10 °C) to reduce the leakage current. Considering the large size of the LAD this can only be achieved passively. For the high-density read-out of the detector dedicated ASICs with very good performance and low power (17 e$^-$ rms noise with 650 μW/channel) are needed. For the M4 configuration, the read-out is performed by 8x 32-channel IDeF-X HD ASICs [25], with A/D conversion carried out by 1x 16-channel OWB-1 ASIC for every detector. The dynamic range of the read-out electronics is required to record events with energy up to 80 keV. The events in the nominal energy range (2-30 keV) are transmitted with 60 eV energy resolution, while those in the "expanded" energy range, 30-80 keV, are transmitted with reduced energy information (2 keV bins) as they will be used to study the timing properties of bright/hard events shining from outside the field of view (e.g., gamma-ray bursts, magnetar flares). The read-out ASICs are integrated on a rigid-flex PCB forming the FEE, with the task of providing: filtered biases to SDD and ASICs, I/O interfaces, mechanical support and interface of the to the Module. The SDD will be back-illuminated, allowing for direct wire-bonding of the anode pads to the ASIC input pads. The flat cable connection to the MBEE is part of the rigid-flex PCB structure. To get full advantage of the compact detector design, a similarly compact collimator design is provided by the mechanical structure of the mature technology of the micro-channel plates, the capillary plate (CP). In the LAD geometry, it is a 5-mm thick sheet of lead-glass (>40% Pb mass fraction) with same size as the SDD detector, perforated by thousands of round micro-pores with 83 μm diameter, limiting the field of view (FoV) to 0.95° (full width at half maximum). The baseline CP plate design and technology adopted for LOFT-M4 is different from that for LOFT-M3. The M4 CP are based on the Hamamatsu round-pore technology. They offer a larger open area ratio (75% vs 70% in M3[2]) and a larger Pb mass fraction. These properties provide improvements in science in terms of a larger effective area and a lower background. In total, the LAD is composed of 1600 SDDs, 1600 CPs and 14 400 ASICs. 1 out 100 Modules is equipped with a "blocked collimator" (the same material and stopping power, but no apertures), for a real-time monitoring of the internal background. The basic unit of the LAD modular design is the Module, designed to be in aluminium as it was in M3. The design proposed for the M4 LAD module remains unchanged.

The LAD panel structure (in Carbon Fiber Reinforced Plastic - CFRP) is the support for the LAD Modules and the PBEE. The key requirements for this structure are to withstand the launch, provide the required mechanical and thermo-elastic stability to the modules (e.g., alignment) and aid the thermal control. To this purpose a common radiator is used on the back side of the Panel composed of an Al honeycomb sandwich with CFRP skins. Twenty modules (total in each panel) are controlled by a single PBEE, located 'underneath' the panel near the hinge to minimise the amount of harness that has to cross the hingeline. The PBEE sends commands to the MBEEs and distributes clocks and power. It receives data (science and HK) from the MBEEs and sends it on to the ICU, which is mounted on the optical bench. The ICU houses the Data Handling Unit (DHU), mass memory and Power Distribution Units (PDU). The DHU receives the data

---

[2] It should be noted that a recent technology development activity carried by ESA demonstrated the feasibility of a 75% open area ratio also with the CP technology adopted for the LOFT-M3 design, as manufactured by Photonis.

from the PBEEs, and formats and compresses this data for telemetry. The ICU manages the PBEEs, handles telecommands (TCs), manages instrument mode and monitors instrument health and performance and interfaces the central Payload Data Handling Unit (PDHU). The LAD experiment is a photon-by-photon experiment with no significant on-board event processing foreseen. The ICU will be based on the LEON3 processor.

Table 1. LAD requirements and anticipated performance.

Parameter	Requirement	Anticipated performance
Effective area	3.2 m^2 at 2 keV 6.4 m^2 at 5 keV 8.0 m^2 at 8 keV 0.8 m^2 at 30 keV	3.8 m^2 at 2 keV (avg 1.5-2.5) 7.8 m^2 at 5 keV 8.5 m^2 at 8 keV 1.1 m^2 at 30 keV
Energy range	2 – 30 keV nominal 30-80 keV extended (for out-FoV events)	1.5 (7.5 σ) lower threshold, 100 keV for maximum energy
Energy resolution in FoR (FWHM, end of life)	240 eV @ 6 keV	180 eV @ 6 keV at the center up to 220 eV at the edge of the FoR (35% sky fraction)
Energy resolution in eFoR (FWHM, end of life)	400 eV @ 6 keV	220 eV @ 6 keV at the center up to 250 eV at the edge of the eFoR (50% sky fraction)
Absolute time accuracy	2 µs	1 µs
Dead time	< 1% @ 1 Crab	< 0.7% @ 1 Crab
Field of View	<1° FWHM	0.95° FWHM
Background	< 10 mCrab	6 mCrab (3 mCrab in 2-10 keV)
Background knowledge	0.25% at 5-10 keV	0.15% at 5-10 keV
Max flux (continuous)	> 500 mCrab	650 mCrab
Max flux (continuous 300 minutes)	15 Crab	15 Crab

The required LAD data transmission is full event information for sources up to 500 mCrab, while increasing data selection (e.g., energy or time histograms) for long and continuous observations of increasing brighter sources is foreseen. An onboard mass memory will allow to store excess telemetry data from observation of sources up to 15 Crab intensity for up to 5 hours, to be gradually downloaded during observations of dim sources (e.g., AGN). The individual event-packet is 24 bits per event. Onboard data storage is foreseen for set-up parameter definition, calibration data and science data (210 GB, for the short observation of very bright sources and in case of ground-pass loss).

The current best estimate of the total LAD mass and power in its M4 configuration is 1103 kg and 868 Watts. A more detailed description of the LAD instrument in its M3 design may be found in [1, 8] and references therein.

3.3 The Wide Field Monitor (WFM)

The WFM is a coded mask camera system with solid state-class energy resolution. This is achieved through the use of the same Silicon Drift Detectors (SDDs) as the LAD, in a modified geometry. Since these detectors provide accurate positions in one direction and only coarse positional information in the other direction, pairs of two orthogonal cameras are used to obtain precise two dimensional source positions. This is illustrated in Figure 6, where the point spread functions of two orthogonal cameras are combined. The useful effective field of view (FoV) of one camera pair is about 70°x70° (90°x90° at zero response). The dimensions of each camera are chosen to match the required sensitivity and the location accuracy. To provide the full required sky coverage, 4 pairs of cameras are foreseen, as shown in Figure 6. The

key instrument requirements are summarized in Table 2 along with the expected performance. With respect to the LOFT-M3 WFM configuration, the Camera design is identical, but the number of Cameras is reduced from 10 to 8 (from 5 to 4 pairs), re-oriented to cover the same FoV. This optimization is based on the large over-compliance of the LOFT-M3 WFM with respect to its scientific requirements, which are unchanged and still satisfied in LOFT-M4.
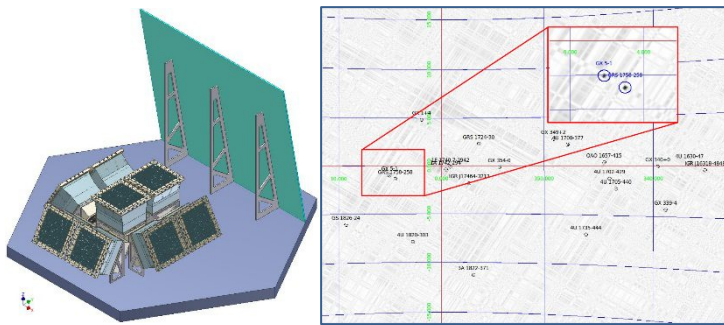

Figure 6. Right: Simulated WFM pointing in the direction of the Galactic Centre. Only a small fraction of the FoV is shown. Left: combination of 4 camera pairs gives the required sky coverage.

Table 2. A listing of some of the key WFM scientific requirements.

Item	Requirement	Anticipated performance
Location accuracy (2D)	< 1 arcmin	< 1 arcmin
Angular resolution (2D)	< 5 arcmin	< 4.3 arcmin
Peak sensitivity in LAD direction (5 σ)	1 Crab (1 s) 5 mCrab (50 ks)	0.6 Crab (1s) 2.1 mCrab (50 ks)
Field of view	3.2 steradian around the LAD pointing	5.5 steradian at zero response, 4.1 at 20% of peak camera response
Energy range	2 – 50 keV	2 – 50 keV
Energy resolution,	500 eV @ 6 keV	< 300 eV @ 6 keV
Energy bands for images	64	$\geq$ 64
Absolute time calibration	2 μs	1 μs
Availability of triggered WFM data	3 hour	< 3 hour
Broadcast of trigger time and position	< 30 s after the event for 65% of the events	< 25 s after the event for 65% of the events

The components of the 8 identical cameras are:

- Pre-tensioned mask, made of Tungsten (0.15 mm thick), with an open area of 25% to optimize the sensitivity for weaker sources. For high imaging quality mask flatness and stability is essential, demonstrated achievable by past experience and extensive thermo-mechanical studies in M3.

- The collimator, supporting the coded mask, is a 3 mm thick CFRP grid structure, covered by a 0.15 mm thick Tungsten sheet, as a background shield. Inner Cu/Mo coating provides fluorescence calibration lines. MLI on the outside improves the thermal stability of the camera.

- The detector tray holds 4 SDDs, each mounted on boards with ASICs and Front End Electronics, with very similar design and functionality as the LAD. However position resolution is important for the WFM, therefore the SDD anode pitch is smaller (145 μm vs 970 μm in the LAD). The required number of ASICs per SDD is higher (28x IDeF-X HD ASICs, with a smaller pitch than LAD, and 2x OWB-1 ASICs). Alignment and stability requirements are stringent and are achieved by design and control of the detector temperature. A 25 μm thick Beryllium window above each SDD protects against micrometeoroid impacts, owing to the large FoV.

- The Back End Electronics (BEE) and Power Supply Unit (PSU) are similar to those used in the LAD, but with additional computing capability of the BEE to determine photon positions. The small anode pitch of the SDDs allows a position resolution of <60 μm along the direction of the anode row. In the drift direction a position resolution of <8 mm is achieved through analysis of the spread of the charge cloud across a group of anodes. Although quite moderate, this is important for limiting potential source confusion in the deconvolved images. The electronics is passively cooled through radiation via the back side of the cameras.

- The Instrument Control Unit (ICU, cold redundant) will control the instrument, interface with the Payload Data Handling Unit (PDHU) and perform the onboard data analysis to identify bright transient sources. The ICU controls each of the 8 cameras independently.

The current best estimate of the total WFM mass and power is 108 kg and 63 Watts.

Flexibility in the LOFT telemetry system allocates any temporarily available bandwidth to WFM data. This will be used to transmit the event-by-event data of the most interesting WFM unit(s) (based on their pointing direction) during, for example, long LAD observations of weaker sources. An average telemetry allocation of ~200 kbit/s, as expected due to the LAD reduced area with respect to LOFT-M3, will allow to transmit all WFM data in photon-by-photon mode, taking full advantage of the intrinsic capability of the instrument. The ICU will employ an onboard capability of locating transient events in real time, in particular gamma ray bursts, with ~1 arcmin accuracy. The time and location of the transient will be transmitted to ground using the onboard VHF system in a ~1 kbit message. The design of the Burst On-board Trigger (LBOT) benefits from the heritage from the SVOM mission concept, as well as past team experience on similar systems on BeppoSAX, HETE-2, AGILE, as well as the INTEGRAL burst alert system.

With the exception of the different read-out ASICs, the design of the individual WFM cameras in the LOFT-M4 design is identical to the LOFT-M3 design. We refer the reader to [1, 9] and references therein for an extensive and comprehensive description.

3.4 The Payload Structure

In contrast to the LOFT-M3 approach, under the proposed M4 design and task share, the Payload Structure is under the responsibility of the payload consortium, as originally proposed for M3. The Payload Structure is composed of the deployment tower, the optical bench (OB) with sunshade, the LAD panels and the deployment mechanisms (Figure 7). The deployment mechanism is composed of deployment hinges, hold-down and release mechanisms (HDRMs) and latches. The current baseline is based on the TAS LOFT-M3 design that, for the smaller number of Modules required by LOFT-M4, results in a shorter and lighter structure.

The Tower is composed of a central cylinder and a set of grid-like panels. The central cylinder is a structural part providing the main load path for axial loads and ensuring stiffness at bending. It is a sandwich cylinder with Al honeycomb and CFRP skins. The set of grid-like panels surround the central tube and, in addition to contribute to the tower stiffness, support the interface points for the HDRMs. The tower height is about 2.7 m to the top of the optical bench (excluding sun shield), whereas the pentagonal footprint has a diameter of about 3.6 m. The OB provides the interface to the deployment mechanism and support for the WFM, the electronics (e.g., ICUs, PDHU, ..) and the WFM sunshield. It also plays a role as radiator. Titanium bracket inserts provide the mechanical I/F to the deployment mechanisms of the LAD panels. The LAD deployment mechanism features two spring actuated and rotary damped hinges per panel, with a mechanical stop and latch. The HDRM, locking the LAD panels to the Tower during launch, is composed of a 5-element set per panel.

The proposed structure for the PLM and its instruments follows the design as proposed at the end of the M3 study phase but downsized in dimension and mass following the reduction in the number of modules. The PLM structure for LOFT-M4 will be developed by CAST, the China Academy for Space Technology. In preparation to the LOFT-M4 proposal, CAST studied the design and technical requirements of the PLM structure and mechanisms, identifying the relevant technology solutions available in China. In Figure 8 a central cylinder structure is shown, compliant with what is required for LOFT and a multitude of inserts. This specific example has a load capacity >5000 kg. A number of similar structures were built for past missions, such as the Lunar Chang'e (1, 2 and 3) missions. Figure 8 also shows two example of hinge and latch mechanism. CAST has a range of hinges available with different load capabilities and with flight heritage.
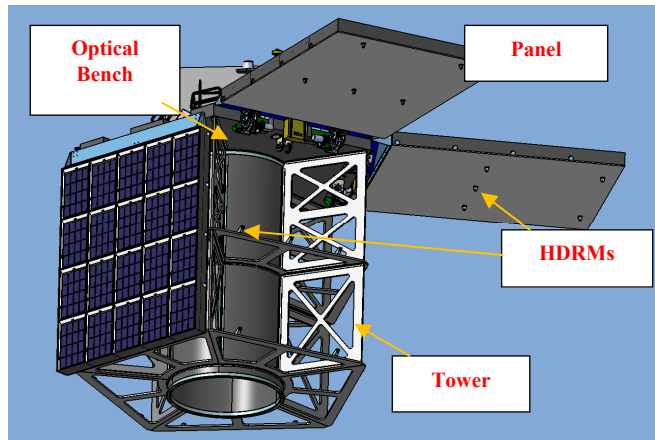
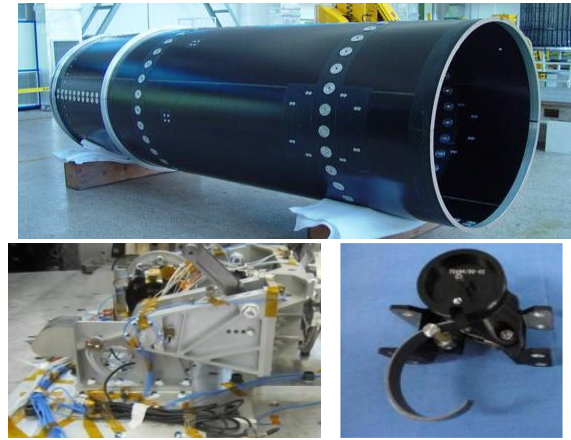Figure 7: PLM structure showing 2 panels deployed and one folded (2 not shown).

Figure 8: Central cylinder with flight heritage.

4. EXPECTED SCIENTIFIC PERFORMANCE

In order to comply with the reduced budget and development schedule announced by ESA in the M4 call, the LOFT-M4 design envisages a LAD instrument composed of 100 modules and a WFM instrument composed of 4 units (8 cameras). The resulting effective area of the LAD and sky coverage of the WFM are shown in Figure 9, where the LAD area – peaking at 8.5 m^2 – is shown in the context of the largest X-ray mission in recent operation or planned, highlighting the enormous improvement. Figure 9 also shows the instantaneous >5 steradian sky coverage enabled by the WFM configuration, together with the 1-year exposure map calculated on the basis of a representative mock-up observing plan.

Despite the 20% reduction in the LAD modules and WFM cameras, the scientific objectives of LOFT-M4 are essentially unchanged with respect to LOFT-M3 and in some cases (e.g., AGN sensitivity) are actually improved, thanks to the lower background offered by the more opaque Hamamatsu collimators. In fact, as discussed in [2], during the LOFT-M3 study a sensitivity analysis was carried out to assess the robustness of the mission and payload design, identifying the impact of potential losses of instrument performance during the mission lifetime. The key parameters are: effective area, spectral resolution, sky visibility, mission duration. The dependence on the effective area is slow and smooth: the M3 study showed that the same core science objectives can be reached with a ~20% smaller instrument by extending the observing time (from 25% to 56%, depending on the specific objectives, with some caveats – see below). Considering the large margins in the available observing time for the Core science, the LAD effective area requirement in LOFT-M4 could be thus revised to 8 m^2 as compared to the 9.5 m^2 of LOFT-M3, effectively optimizing of the mission resources. In fact, based on a detailed analysis, the total observing time required for the core science goals is 33.7 Ms (it was 25 Ms for LOFT-M3). Considering Earth occultation, calibration exposures, thermal and AOCS relaxation times, etc., an observing availability of 60% was estimated by industries in M3, meaning that the Core Science requires less than 1.8 years and ~40% of the 3-year LOFT total net observing time (56.8 Ms) is available for the Observatory Science, plus any mission extension. For goal "SFG3" ("detect kHz QPOs at their coherence time, measure the waveforms and quantify the distortions due to strong field GR effects") a smaller effective area implies a smaller number of available sources, reducing from 10 to 8-9, which is still acceptable. For "SFG5" ("Fe profiles in supermassive black holes") the improved background enabled by the new M4 collimator leads to over-compensating the loss, allowing SFG5 studies on more sources than planned in LOFT-M3.

For what concerns the WFM, the M3 design was actually significantly over-performing its scientific requirements, especially in terms of sensitivity as a function of the FoV. By a different arrangement of the WFM units (Figure 6) the same sky coverage could be achieved, with a sensitivity still compliant with the original M3 scientific requirements.
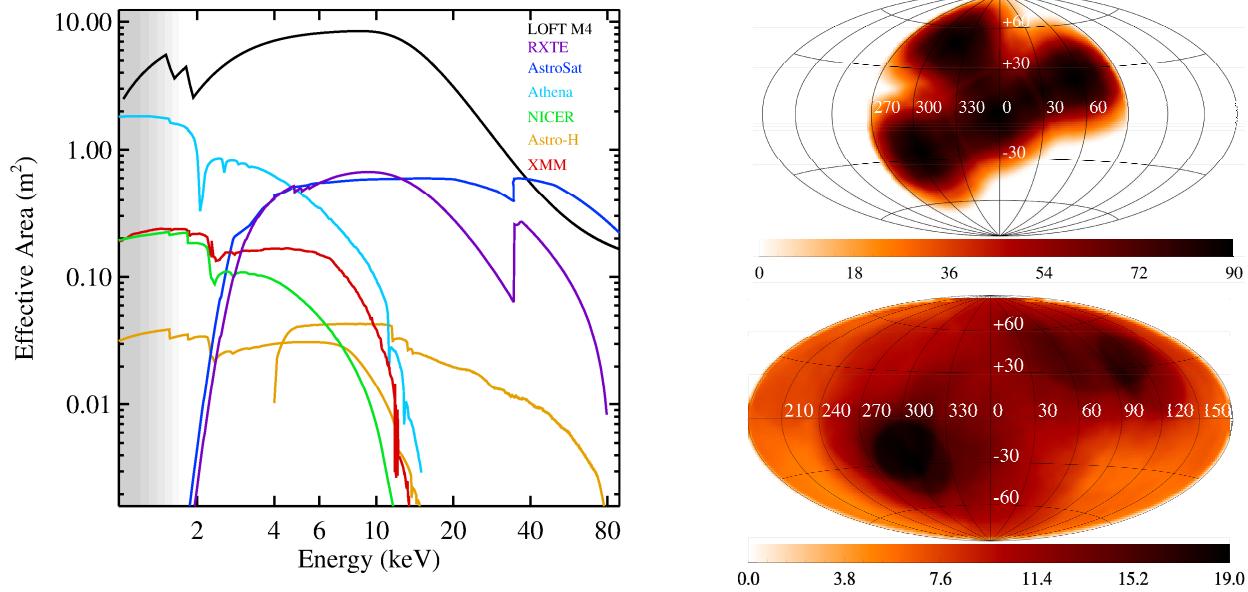
Figure 9. Left: The effective area of LOFT/LAD as compared to the largest past, on-going and approved missions. The shaded area below 2 keV indicates the fact that the LAD will outperform its science requirement of 2 keV low energy threshold, by extending its sensitivity down to ≤ 1.5 keV, beneficial to the study of complex absorption structures. Right: Map in Galactic coordinates of the active detector area for a sample observation performed in the direction of the Galactic centre (top) and 1yr Exposure map in Galactic coordinates for positions covered by at least 10 cm^2 per observation. Map scale is given in Ms.

As examples of the LOFT scientific performance in its M4 configuration, in Figure 10 we report results expected through LOFT observations. In particular, the left panel shows the mapping of the NS equation of state in the M-R diagram as achieved through the pulse profile modeling of a realistic sample of ~10 NS. The statistical accuracy and the control of the systematic uncertainties will allow LOFT to precisely map the correct EoS. For the strong field gravity science case, the panel on the right shows a realistic simulation of the accuracy with which LOFT will determine the iron line distortions in supermassive black holes in the time domain. Orbital radius r/r_g is measured to ±1-2% and given spin, BH mass to ≲±30%. Any narrow lines in the profile drop out of these differential measurements: arising at large radii, these lines vary slowly. Various other tomographic studies will be performed at unprecedented S/N (e.g., eclipse mapping; see [12]).

5. FUTURE PERSPECTIVES

The M3 study demonstrated the technical and programmatic feasibility of the LOFT mission within the boundary conditions of an ESA M-class mission. The design optimization proposed in M4 was again assessed by ESA to be compliant with the reduced M4 budget and its faster schedule. The LOFT science was again highly ranked in the M4 selection process, confirming the M3 scientific evaluation. LOFT was actually short-listed to the last 5-proposal down-selection, but eventually did not make it to the final list of 3 M4 mission candidates, currently under their assessment study. The LOFT Consortium remained active though, working towards the M5 ESA mission call and collaborating with international partners on mission concepts led by other agencies and incorporating part of all of the LOFT science objectives and instrumentation. In particular, the eXTP mission concept [26] is being studied by the Chinese Academy of Sciences for a target launch date earlier than 2025 and it now includes a substantial participation of the LOFT Consortium and LOFT instrumentation. In addition to that, the LOFT-P mission concept [27] is a study showing the feasibility of the LOFT mission within the context of the NASA Probe-class missions, potentially starting their development within the Decadal Survey 2020 context, for a launch in the late 2020's. It is yet undecided whether the LOFT Consortium will re-submit the LOFT mission proposal to the ESA M5 competition or will instead only focus on the development of the eXTP and LOFT-P mission concepts.
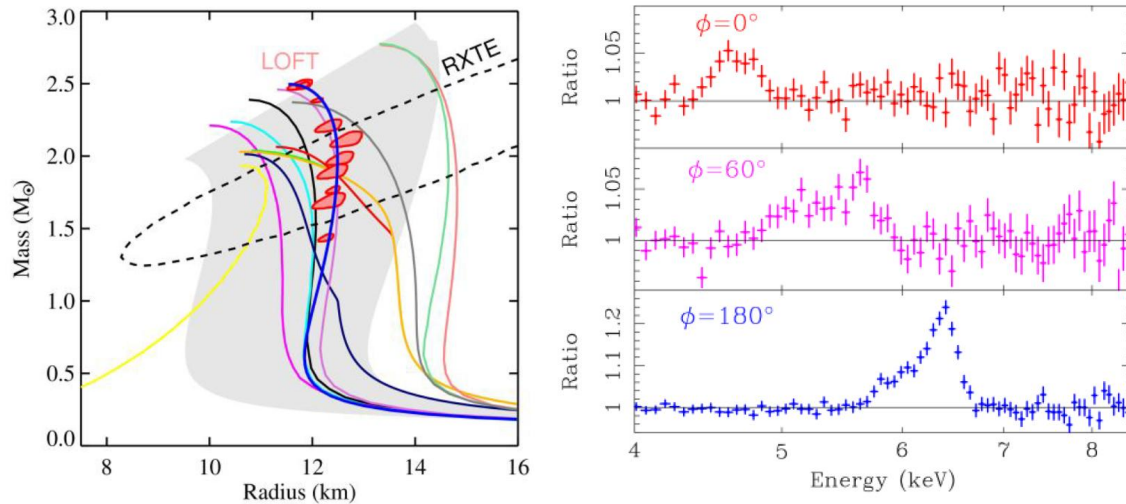
Figure 10. Left: LOFT measurements (red error regions) tightly constrain the dense matter EOS. The models (curves) illustrate current theoretical predictions for the EOS. A representative RXTE error region is shown.. Right: Fluorescent line profile ratios to line average from two 10-ks, $10r_g$ orbits of a hot spot around a 10^7 M_o spin 0.5 black hole. Spot contributes 10% of the line flux in a 2 mCrab AGN for a total of 20 ks (~3 ks per profile plotted). Disk inclination 30°.

ACKNOWLEDGEMENTS

REFERENCES

[1] LOFT Assessment Study Report (Yellow Book), Dec. 2013: http://sci.esa.int/loft/53447-loft-yellow-book/
[2] LOFT Science Requirements Document, Sept. 2013: http://sci.esa.int/loft/49447-loft-science-requirements-document/
[3] LOFT Payload Definition Document, Oct. 2012: http://sci.esa.int/loft/49448-loft-payload-definition-document/
[4] LOFT Mission Requirements Document, Feb. 2013: http://sci.esa.int/loft/51295-loft-mission-requirements-document/
[5] LOFT Preliminary Requirements Review Technical and Programmatic Report, Dec.2013: http://sci.esa.int/loft/53521-loft-preliminary-requirements-review-technical-and-programmatic-report/
[6] Feroci et al. 2012, Experimental Astronomy, Volume 34, Issue 2, pp 415-444.
[7] Feroci et al. 2014, Proc. SPIE Space Telescopes and Instrumentation 2014 Vol. 9144, 91442T-1
[8] Zane et al. 2014, Proc. SPIE Space Telescopes and Instrumentation 2014, Vol. 9144, 91442W-1
[9] Brandt et al. 2014, Proc. SPIE Space Telescopes and Instrumentation 2014, Vol. 9144, 91442V
[10] Watts et al. 2016, Review of Modern Physics, Vol. 88, 021001-1.
[11] Uttley et al. 2014, The Astronomy and Astrophysics Review, Volume 22, article id.72
[12] White Paper 1: "Accretion, ejection and reprocessing in supermassive black holes", De Rosa, A.; Bianchi, S.; Giroletti, M. Marinucci, A.; Paolillo, M.; Papadakis, I. Risaliti, G.; Tombesi, F.; Cappi, M.; Czerny, B. Dadina, M.; De Marco, B.; Dovciak, M.; Karas, V. Kunneriath, D.; La Franca, F.; Manousakis, A. Markowitz, A.; McHardy, I.; Mehdipour, M. Miniutti, G.; Paltani, S.; Perez-Torres, M. Peterson, B.; Piconcelli, E.; Petrucci, P. O. Ponti, G.; Rozanska, A.; Salvati, M.; Sobolewska, M. Svoboda, J.; Trevese, D.; Uttley, P.; Vagnetti, F.Vaughan, S.; Vignali, C.; Vincent, F. H. Zdziarski, A., http://arxiv.org/abs/1501.02768

[13] White Paper 2: "The study of neutron star magnetospheres with LOFT",Mignani, R. P.; Bocchino, F.; Bucciantini, N. Burgay, M.; Cusumano, G.; De Luca, A.; Esposito, P. Gouiffes, C.; Hermsen, W.; Kanbach, G.; Kuiper, L. Israel, G. L.; Marelli, M.; Mereghetti, S. Mineo, T.; Motch, C.; Pellizzoni, A.; Possenti, A. Ray, P. S.; Rea, N.; Rudak, B.; Salvetti, D. Shearer, A.; Slowikowska, A.; Tiengo, A. Turolla, R.; Webb, N., http://arxiv.org/abs/1501.02773

[14] White Paper 3: "The LOFT perspective on neutron star thermonuclear bursts", in 't Zand, J. J. M.; Altamirano, D. Ballantyne, D. R.; Bhattacharyya, S.; Brown, E. F. Cavecchi, Y.; Chakrabarty, D.; Chenevez, J. Cumming, A.; Degenaar, N.; Falanga, M. Galloway, D. K.; Heger, A.; José, J.; Keek, L. Linares, M.; Mahmoodifar, S.; Malone, C. M. Méndez, M.; Miller, M. C.; Paerels, F. B. S. Poutanen, J.; Rózanska, A.; Schatz, H.; Serino, M. Strohmayer, T. E.; Suleimanov, V. F. Thielemann, F.-K.; Watts, A. L.; Weinberg, N. N. Woosley, S. E.; Yu, W.; Zhang, S.; Zingale, M., http://arxiv.org/abs/1501.02776

[15] White Paper 4: "The physics of accretion-ejection with LOFT", Casella, P.; Fender, R.; Coriat, M.; Kalemci, E. Motta, S.; Neilsen, J.; Ponti, G.; Begelman, M. Belloni, T.; Koerding, E.; Maccarone, T. J. Petrucci, P.-O.; Rodriguez, J.; Tomsick, J. Bhattacharyya, S.; Bianchi, S.; Del Santo, M. Donnarumma, I.; Gandhi, P.; Homan, J.; Jonker, P. Kalamkar, M.; Malzac, J.; Markoff, S.; Migliari, S. Miller, J.; Miller-Jones, J.; Poutanen, J. Remillard, R.; Russell, D. M.; Uttley, P. Zdziarski, A., http://arxiv.org/abs/1501.02766

[16] White Paper 5: "Probing the emission physics and weak/soft population of Gamma-Ray Bursts with LOFT" Amati, L.; Stratta, G.; Atteia, J.-L. De Pasquale, M.; Del Monte, E.; Gendre, B.; Götz, D. Guidorzi, C.; Izzo, L.; Kouveliotou, C.; Osborne, J. Penacchioni, A. V.; Romano, P.; Sakamoto, T. Salvaterra, R.; Schanne, S.; in 't Zand, J. J., M. Antonelli, L. A.; Braga, J.; Brandt, S. Bucciantini, N.; Castro-Tirado, A.; D'Elia, V. Feroci, M.; Fuschino, F.; Guetta, D.; Longo, F. Lyutikov, M.; Maccarone, T.; Mangano, V. Marisaldi, M.; Mereghetti, S.; O'Brien, P. Rossi, E. M.; Ryde, F.; Soffitta, P.; Troja, E. Wijers, R. A. M. J.; Zhang, B., http://arxiv.org/abs/1501.02772

[17] White Paper 6: "High-energy radiation from thunderstorms and lightning with LOFT", Marisaldi, M.; Smith, D. M.; Brandt, S. Briggs, M. S.; Budtz-Jørgensen, C.; Campana, R. Carlson, B. E.; Celestin, S.; Connaughton, V. Cummer, S. A.; Dwyer, J. R.; Fishman, G. J. Fullekrug, M.; Fuschino, F.; Gjesteland, T. Neubert, T.; Østgaard, N.; Tavani, M., http://arxiv.org/abs/1501.02775

[18] White Paper 7: "Stellar flares observed by LOFT: implications for the physics of coronae and for the space weather environment" of extrasolar planets, Drake, S. A.; Behar, E.; Doyle, J. G.; Güdel, M. Hamaguchi, K.; Kowalski, A. F.; Maccarone, T. Osten, R. A.; Peretz, U.; Wolk, S. J., http://arxiv.org/abs/1501.02771

[19] White Paper 8: "Probing stellar winds and accretion physics in HMXBs and ULXs with LOFT", Orlandini, M.; Doroshenko, V.; Zampieri, L.; Bozzo, E.; Baykal, A.; Blay, P.; Chernyakova, M.; Corbet, R.; D'Aì, A.; Enoto, T.; Ferrigno, C.; Finger, M.; Klochkov, D.; Kreykenbohm, I.; Inam, S. C.; Leyder, J.-C.; Jenke, P.; Masetti, N.; Manousakis, A.; Mihara, T.; Paul, B.; Postnov, K.; Reig, P.; Romano, P.; Santangelo, A.; Shakura, N.; Staubert, R.; Torrejón, J. M.; Walter, R.; Wilms, J.; Wilson-Hodge, C., http://arxiv.org/abs/1501.02777

[20] White Paper 9: "LOFT as a discovery machine for jetted Tidal Disruption Events", Rossi, E.M.; Donnarumma, I.; Fender, R.; Jonker, P. Komossa, S.; Paragi, Z.; Prandoni, I.; Zampieri, L., http://arxiv.org/abs/1501.02774

[21] White Paper 10: "Dissecting accretion and outflows in accreting white dwarf binaries", de Martino, D.; Sala, G.; Balman, S.; Bernardini, F. Bianchini, A.; Bode, M.; Bonnet-Bidaud, J.-M. Falanga, M.; Greiner, J.; Groot, P.; Hernanz, M. Israel, G.; Jose, J.; Motch, C.; Mouchet, M. Norton, A. J.; Nucita, A.; Orio, M.; Osborne, J. Ramsay, G.; Rodriguez-Gil, P.; Scaringi, S. Schwope, A.; Traulsen, I.; Tamburini, F., http://arxiv.org/abs/1501.02767

[22] White Paper 11: "Binary evolution with LOFT", Maccarone, T. J.; Wijnands, R. A. M.; Degenaar, N. Archibald, A.; Watts, A.; Vaughan, S.; Wynn, G. Knevitt, G.; Farr, W.; Andersson, N. van der Klis, M.; Patruno, A; Tauris, T., http://arxiv.org/abs/1501.02769

[23] White Paper 12: "The innermost regions of relativistic jets and their magnetic fields in radio-loud Active Galactic Nuclei", Donnarumma, I.; Agudo, I.; Costamante, L. D'Ammando, F.; Giovannini, G.; Giommi, P. Giroletti, M.; Grandi, P.; Jorstad, S. G. Marscher, A. P.; Orienti, M.; Pacciani, L. Savolainen, T.; Stamerra, A.; Tavecchio, F. Torresi, E.; Tramacere, A.; Turriziani, S. Vercellone, S.; Zech, A., http://arxiv.org/abs/1501.02770

[24] Rachevski et al. 2014, JINST 9, P07014

[25] Gevin et al. 2012, NIM A 695, 415

[26] Zhang et al. 2016, These proceedings

[27] Wilson-Hodge et al. 2016, These proceedings